Available online at www.sciencedirect.com
SCIENCE DIRECT®
Tetrahedron: Asymmetry
Tetrahedron: *Asymmetry* 15 (2004) 2345–2350

A drop of enantioselectivity in the *Pseudomonas cepacia* lipase-catalyzed ester hydrolysis is influenced by the chain length of the fatty acid

Andrea Tafi,[a] Fabrizio Manetti,[a] Maurizio Botta,[a,*] Silvana Casati[b] and Enzo Santaniello[b,*]

[a]*Dipartimento Farmaco Chimico Tecnologico, Università degli Studi di Siena, Via Aldo Moro, 2 I-53100 Siena, Italy*
[b]*Dipartimento di Scienze Precliniche L.I.T.A.-Vialba, Università degli Studi di Milano, via G. B. Grassi,74 I-20157 Milano, Italy*

Received 7 May 2004; accepted 10 June 2004
Available online 23 July 2004

Abstract—A two-step molecular mechanics based computational procedure has been applied to explain the enantioselectivity observed in the hydrolysis of esters of primary alcohols, carried out in the presence of a lipase from *Pseudomonas cepacia*. This approach proved to be very effective in explaining an unpredictable drop in enantioselectivity, experimentally observed when the chain of the fatty acid was lengthened and to predict the chain length in correspondence of which the effect should have revealed itself.

1. Introduction

The enantioselectivity of lipases is still mainly rationalized by using computational approaches exploiting molecular mechanics (MM) related methods. Mixed quantum mechanics/molecular mechanics (QM/MM) methods have recently been applied with success to rationalize the enantioselectivity of specific enzymes.[1] However MM approaches are still attractive in modelling enzyme reactivity, despite their theoretical limitations, due to their speed, flexibility, and reliability.[2] Various models have been proposed over the last 10 years, with the aim of rationalizing or predicting the behavior of several lipases towards their substrates.[3] In particular, the enantioselectivity and substrate specificity of the lipase from *Pseudomonas cepacia* (PcL) has been thoroughly studied and interpreted.[4]

The MM computational protocol, which is the most commonly applied, consists of conformational searches or molecular dynamics (MD) simulations to model the lowest-energy tetrahedral intermediate (THI) formed by each enantiomer (the fast- and the slow-reacting one) over the course of a studied reaction, assuming that this is a good mimic of the effectively relevant transition state. Through such an approach,[4a] Tuomi and Kazlauskas were able to discuss the enantioselectivity of PcL towards esters of primary alcohols in terms of competing recognition (experimentally evaluated by the Michaelis–Menten constant) and reaction rate differences between enantiomers. These authors, however, pointed out that their modelling could better account for competing recognition. A pure THI model, which is focused on the location of the lowest-energy structure, does not favor a proper kinetic interpretation of the enantioselectivity, based on the height of the energy barrier in correspondence of the transition state (TS), as it causes a rather thermodynamic perspective, based on the depth of the tetrahedral intermediate's energy hollow. The practical limitations of the pure THI approach have been recently reported[4e] and consequently, a 'pseudomolecular dynamics under constraints' protocol has been proposed with the aim of advancing the THI modelling strategy.

A different kinetic approach, based on Deslongchamps' stereoelectronic theory[5] and theoretically verified by QM calculations, was proposed and firstly applied in 1998 to rationalize the enantioselectivity of lipases.[6] According to Ema's studies, conformational requirements at the reacting center come into play in

* Corresponding authors. Tel.: +39-0577-234-306; fax: +39-0577-234-333 (M.B.); tel.: +39-02-503-19693; fax: +39-02-382-10295; e-mail addresses: botta@unisi.it; enzo.santaniello@unimi.it

0957-4166/$ - see front matter
doi:10.1016/j.tetasy.2004.06.010

correspondence to the transition state leading to the formation of the first THI and are responsible for the enantioselective effect, by modulation of the reaction's activation energy. Repulsive interactions or steric clashes inside the active site allow[7] only one enantiomer to get to the TS's theoretically favored conformation (*gauche* with respect to the $C–O_{alcohol}–C–O_{serine}$ dihedral angle); as a consequence, an energy gap of a few kcal mol^{-1} is created between the two competing TSs.[6] Notably, the stereoelectronic theory allows such thermodynamic concepts to be transformed into geometric constraints (reflecting the energy difference between the diastereomeric forms of the transition states) on the three-dimensional structure of the THIs. Accordingly, *gauche*, rather than *anti* conformations, must be adopted by the tetrahedral intermediates to follow a low activation energy reaction pathway.[6,8]

A novel two-step MM based modelling procedure has recently been developed and successfully tested to explain the enantioselectivity observed in the hydrolysis of esters of secondary alcohols in the presence of PcL.[4b] This method exploits Ema's results to involve the stereoelectronic theory concepts into a MM approach, which simulates the two main steps (recognition and THI formation) of the lipase catalyzed reactions. For a given substrate, docking studies enable us to detect potentially productive Michaelis–Menten (M–M) complexes of both enantiomers, which in turn are converted into tetrahedral intermediates. After geometric optimization of the latter, the stereoelectronic theory constraints are used as an acceptance test, in order to explain or predict the course of the simulated reaction. Hereafter, this procedure will be named the 'Essential Pathway Approach' (EPA).

Herein, EPA is applied for the first time to explain results obtained from the hydrolysis of racemic mixtures of esters of 3-phenyl-2-methyl-1-propanol (compound **1a**, Fig. 1), performed in aqueous medium, in the presence of PcL. Moreover, the original computational procedure has been further improved by the adjustment of an energy minimization protocol,[9] which has allowed the evaluation of the steric energy of enzyme–substrate complexes.

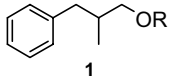

1

a. R=H
b. R=$COCH_3$
c. R=$CO(CH_2)_2CH_3$
d. R=$CO(CH_2)_6CH_3$
e. R=$CO(CH_2)_{10}CH_3$
f. R=$CO(CH_2)_4CH_3$

Figure 1. Structure of esters considered as substrates for PcL-catalyzed hydrolysis reactions.

2. Results and discussion

Compound **1a** is a primary alcohol whose stereochemical outcome in the PcL-catalyzed transesterification[10] has been studied in detail from a MM point of view.[4a,11] We observed (see Table 1 and the Experimental) that the excellent enantioselectivity of the PcL-catalyzed hydrolysis of esters **1b** and **1c** dramatically fell when the chain of the fatty acid was lengthened to esters **1d** and **1e**. The experimental results shown in the Table suggest that the extension of the acyl chain could produce a perturbation on the reaction pathway nullifying the enantiopreference shown by the enzyme towards the (*S*)-enantiomers of compounds **1b** and **1c**. With the aim of clarifying this unpredictable effect at a molecular level, the hydrolyses of compounds **1b–e** were simulated and the results obtained for **1b** and **1d**, taken as representative examples of the whole set of compounds, reported here in detail.

Table 1. PcL-catalyzed hydrolysis of esters **1b–f**

Substrate	Time (h)	% Conv.[a]	Eep[b]	E[c]
1b	2	32	>98	>100
1c	2	27	>98	>100
1d	7	24	16	1.4
1e	4	26	25	1.8
1f	3	32	80	13

[a] Determined by GC.
[b] Evaluated by 1N NMR analysis of the corresponding MTPA esters, according to Dale et al.[12]
[c] Determined according to Chen et al.[13]

EPA was first applied to acetate **1b**. The docking found a quite similar recognition geometry for both enantiomers of this substrate into the active site of PcL (corresponding as a whole to an alignment already described for the same compound[4a,11]). In particular, the orientation in 3D space of the hydrogen and methyl groups at the stereocenter (showing roughly exchanged positions) appeared to be the only difference in the recognition of the two enantiomers of **1b** by PcL. This theoretical achievement confirmed again that, even though the enzyme is able to bind in a different way with the two enantiomers of its substrates, the enantioselection of PcL does not come into play during the recognition process.[4,7] In fact, no structural enantioselectivity indicators[4] came out from docking to hint at any chiral discrimination. When the THI of both enantiomers was built and optimized a critical enantioselective differentiation between the two diastereomeric structures occurred, which fully rationalized the experimental result of the hydrolysis reaction of this compound.[4b,6,7] In the case of (*S*)-**1b**, the methyl group at the stereocenter was easily accommodated inside a small hydrophobic pocket of PcL, formed by residues His86, His286, Leu287, and Ile290,[4a,b,13] allowing the THI to adopt the expected productive *gauche* conformation displayed in red in Figure 2. In the case of (*R*)-**1b** (yellow in Fig. 2), even though the overall orientation of the M–M complex was maintained, an unproductive *anti*-conformation of the THI was adopted, that prevented the methyl group to be directed completely outwards with respect to the small cavity mentioned above and to be totally solvent exposed.

EPA was then applied to the octanoate **1d** (see Fig. 3).

The study of the recognition of both enantiomers of this substrate by PcL did not exhibit any relevant novelty with respect to the corresponding enantiomers of **1b**.

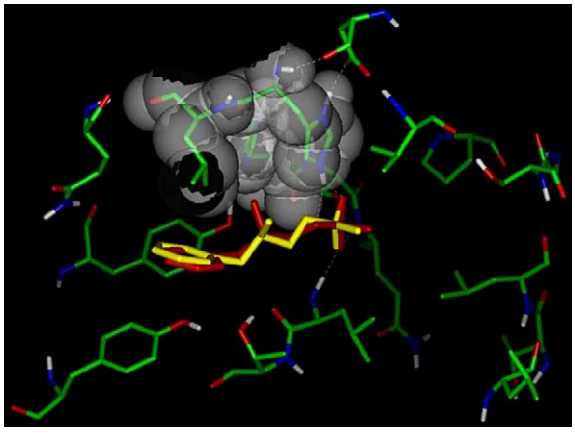

Figure 2. Superimposition of the calculated tetrahedral intermediates of (*S*)-**1b** (red) and (*R*)-**1b** (yellow) located at their proper respective 3D positions inside the active site of PcL. Hydrogen atoms bound to heteroatoms are displayed. For the sake of simplicity, only residues useful for the discussion are shown. The surface of the pocket formed by residues His86, His286, Leu287, and Ile290 is shown in transparency.[14]

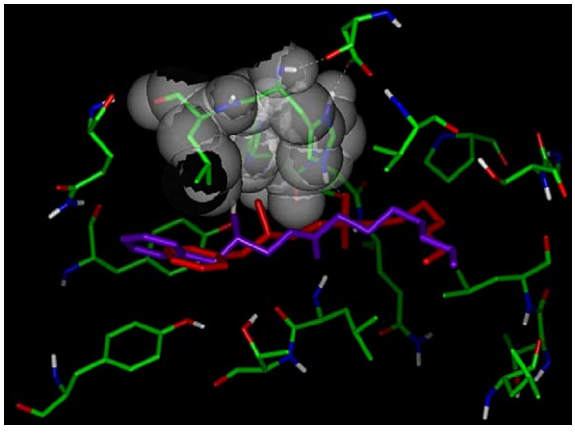

Figure 3. Superimposition between calculated recognition geometry (violet) and tetrahedral intermediate (red) of (*S*)-**1d**, located at their proper respective 3D positions inside the active site of PcL. The fatty acid chain occupies, folded, the HA binding pocket in the right side of the figure.[14]

The common alcoholic moieties were found to be perfectly superimposable with each other [(*R*)-**1b** with (*R*)-**1d** and (*S*)-**1b** with (*S*)-**1d**] as expected, while the achiral fatty acid chain of both enantiomers of **1d** was folded (one C–C–C–C torsion value was approximatively equal to 60°) to occupy the so called HA binding pocket, 'a hydrophobic, well defined groove that is the binding site for the sn-3 fatty acid chain of a phosphonate triacylglycerol analogue inhibiting PcL'.[15] When the THI of both enantiomers of **1d** was optimized (starting from their respective lowest energy M–M complexes), while the binding of the alcoholic moieties followed the same pattern of **1b** (shown in Fig. 2), a remarkable conformational interconversion of the fatty acid chain occurred, involving in a non-enantioselective manner both diastereomeric enzyme–substrate complexes. The case of (*S*)-**1d** is shown in Fig. 3: the formation of the covalent bond between the catalytic serine residue and the carbonyl carbon of the substrate forces the latter to approach PcL. Consequently, the acyl moiety must rearrange into HA, crossing torsional energy barriers and adopting a conformation more folded and higher in energy, than the one displayed by the M–M complex (three C–C torsion values were found to differ from 180° and 60°).

In the light of the above reported computational results, it was hypothesized that the refolding of the fatty acid chain inside HA might produce a compulsory increase in the activation energy of the rate-determining step (the one leading to the first tetrahedral intermediate). This would be effective on both enantiomers and be able to cancel out any reaction rate difference between them, otherwise referable to the exclusive possibility of the (*S*)-enantiomer to take a *gauche* TS conformation.[16] According to this hypothesis, any longer acyl chain may directly agitate the system determining a new bottleneck in the reaction pathway irrespective of the stereochemistry of the reacting substrate.

With the aim of supporting such an assumption (based on structural considerations) free energy differences between the complexes with PcL of the (*R*)- and (*S*)-enantiomers were roughly estimated.[9,17] The values obtained for compounds **1b**–**f**, at both recognition and THI formation steps, are shown in Table 2.

Table 2. Steric energy differences (kJ/mol) between PcL-enantiomer (*S* and *R*) complexes, calculated for different substrates

Substrate	$\Delta E(R,S)$[a] M–M[b]	$\Delta E(R,S)$[a] THI[c]
1b	6.7	−5.9
1c	5.3	−4.0
1d	5.2	0.9/6.0[d]
1e	6.0	−1.4/0.3[e]
1f	4.0	2.0

[a] $\Delta E(R,S) = E(\text{PcL-}S) - E(\text{PcL-}R)$.
[b] Calculated at the recognition step (M–M complexes).
[c] Calculated at the THI formation step.
[d] Dependent on the conformation of the alcoholic moiety of the THI of (*S*)-**1d** (0.9 *gauche*; 6.0, *anti*).[16]
[e] Dependent on the conformation of the alcoholic moiety of the THI of (*S*)-**1e** (−1.4 *gauche*; 0.3, *anti*).[16]

Although the accuracy of the differences reported in Table 2 could be controversial for the approximations used in their calculation (the constraints imposed during the minimizations), the comparison among these values proved to be useful in estimating, in a qualitative manner, the enantioselective behavior displayed by PcL in the hydrolysis reaction of the studied substrates. In particular, the trend of the ΔE values calculated in correspondence of the THI formation (third column in the table) correctly confirms both the advantage of (*S*)-**1b** with respect to (*R*)-**1b** in their hydrolysis in presence of PcL (stereoelectronic requirements) and the drop in enantioselectivity experimentally observed going from **1b** to **1d**, determined by the extension of the fatty acid chain (overflowing conformational rearrangement).[18]

3. Conclusion

The robustness of the model proposed herein to rationalize the behavior of PcL towards compounds **1b–d** was tested through the prediction of the fatty acid chain length, in correspondence of which the drop of enantioselectivity should have revealed itself. The simulation of the hydrolysis of the hexanoate **1f** was performed and it was predicted that PcL should have hydrolyzed this compound with lower enantioselectivity than **1b** and **1c**, as suggested by both the folding of the acyl chain into HA (results not shown) and the $\Delta E(R,S)$ THI values (Table 2). The experimental outcome of the hydrolysis of **1f** confirms the prediction (see Table 1), thus demonstrating the reliability of our computational approach.

4. Experimental

4.1. PcL-catalyzed hydrolysis of esters 1b–f

The highly enantioselective enzyme catalyzed hydrolyses of acetate **1b** and butyrate **1c** proceeded in absence of surfactant that was required for the hydrolysis of less soluble longer chain esters. In a separate experiment, we observed that the addition of Triton X 100 to these enzymatic reactions did not influence the *E* values of the hydrolysis of **1b** and **1c**, which remained >100. For the sake of homogeneity, we herein report the experimental protocol for all substrates in the presence of Triton X 100.

To a suspension of the ester (0.8 mmol) in a phosphate buffer (0.05 M at pH 7, 2 mL) under magnetic stirring, Triton X 100 (50 mg) and PcL (Amano, 30 U/mg, 16 mg) were sequentially added. The reaction was continuously monitored by a pH meter with the pH kept at 7 by adding 0.1 M NaOH. When the required conversion was reached, 1 M HCl and NaCl were added, the reaction mixture extracted with dichloromethane (3×5 mL) and dried over Na_2SO_4. Alcohol **1a** was purified by silica gel column chromatography (petroleum ether/acetate, 8:2).

4.2. Preparation of the enzyme starting structure

The coordinates of Pseudomonas cepacia lipase (PcL) utilized in this study were collected from the structure with entry number 3LIP in the Brookhaven Protein Data Bank.[19] The 'enzyme starting structure' to be used in all computations was prepared as follows. The coordinates of PcL were red into the software package MacroModel/BatchMin (version 5.5)[20] equipped with the Amber* united atoms force field.[21] Accordingly to this choice, hydrogen atoms were added to heteroatoms only. Bound water molecules were maintained throughout the calculations with the exception of four located at the active site cleft, which were removed to prevent hindrance to the docking of substrates. The generalized Born solvent-accessible surface area (GB/SA) continuum solvation method of BatchMin was applied to simulate the effects of water.[22] Amber* and GB/SA water were used for all of the subsequent calculations. 3LIP was first minimized until a 1×10^{-1} kJ mol^{-1} Å^{-1} gradient value was reached, after having fixed all the backbone atoms at their crystallographic positions in 3D space. The output structure was then subjected to a step-wise simulated annealing protocol (applying the same set of constraints to the backbone atoms as in the preliminary minimization and the SHAKE algorithm) to allow both side chains and water molecules to mutually relocate in such a way as to optimize their mutual interactions. A 10 ps molecular dynamics (MD) run was firstly performed at 300 K with a 1.5 fs time step for equilibration purposes. The next MD run lasted 150 ps with the same time step, during which the system was slowly cooled to approximately 150 K. The third and final MD run had the system cooled to 50 K over 20 ps with a 2.0 fs time step. Finally, the output structure was reminimized by applying the above described set of constraints.

4.3. Flexible docking of the substrates and construction of their tetrahedral intermediates.[4b]

Three-dimensional structures of compounds (*R*)-**1b**, (*R*)-**1c**, (*R*)-**1d**, (*R*)-**1e**, (*R*)-**1f**, (*S*)-**1b**, (*S*)-**1c**, (*S*)-**1d**, (*S*)-**1e**, and (*S*)-**1f** were constructed and optimized in MacroModel/BatchMin. The BatchMin Monte Carlo Multiple Minimum methodology (MCMM command) was then chosen to carry out simulations involving 10,000 steps, in which each substrate (guest compound) was subjected to a flexible docking into PcL (host compound). BatchMin command MOLS permitted us to perform rotations and translations of the guest, with a maximum value of the random rotational angle equal to 180° and a maximum allowed translation movement of 6.0 Å at each step. At the same time, the compound was subjected to a statistical conformational search inside the active site of PcL by random changes in the torsion angles of all its rotatable bonds (4 in the simplest case of **1b**, up to 12 in the case of **1e**) as given by the TORS command. Values of 30° and 180°, respectively, were chosen as the minimum and maximum angular increment to be added or subtracted at each Monte Carlo step. Each docking simulation was repeated a few times starting from different arbitrary geometries to produce a complete sampling of the whole potential energy hypersurface of the selected PcL-substrate system. Energy minimizations of the output structures that satisfied three distance constraints (distance between the carbonyl carbon of the guest and the oxygen atom (O_γ) of Ser87 were shorter than 4.5 Å; distances between the carbonyl oxygen of the guest and the backbone NHs of Leu17 and Gln88 were shorter than 4.5 Å) were carried out in order to obtain eligible Michaelis–Menten (M–M) complexes. BatchMin least square superimposition routine (COMP command) was selected to eliminate duplicate minima and the global chirality checking command (CHIG) was used to reject any structure whose chirality had been changed by the minimization. Due to the large number of atoms in the whole system, a region of PcL surrounding the active site cleft was selected, which comprised of 71 residues plus 10 crystal water molecules for a total of 692 atoms. All calcula-

tions were performed on this internal subset, while the external residues and water molecules were not included in the calculations.

Two further restraints were imposed in order to maintain the 3D structure of the enzyme largely unmodified during the docking simulations:

(a) the side chains of 18 residues inside the subset (namely Leu17, Thr18, Tyr23, Tyr29, His86, Ser87, Ser117, Ph119, Val123, Leu164, Leu167, Asp264, Val266, Val267, His286, Leu287, Glu289, Ile290) and four water molecules (W465, W501, W510, W532), either localized on the walls of the active site cleft or connected to residues playing a role in the catalytic reaction, were fully minimized together with the guest in order to guarantee the balance between the surfaces of the two partners;
(b) all the other atoms of the internal subset were fixed in 3D space even if their nonbonded interactions with all the relaxing atoms were calculated.

The distance between the hydroxyl hydrogen atom of the Ser87 and the adjacent N_ε atom of His286, as well as the distance between the hydrogen of imidazole NH of His286 and the carboxylate ion of Asp264, were monitored during the docking simulations to ensure that the relative orientations of the residues of the catalytic triad were compatible with the mechanism of the hydrolytic reaction.

Families of the lowest energy output docking geometries were transformed into the tetrahedral intermediates: one long covalent bond was drawn between the Ser87 O_γ oxygen atom and the carbonyl carbon atom of the different compounds while transferring one H atom from Ser87 to His286 (deletion and drawing of one bond without modifying the position of the atom). Finally the carbonyl group of the substrates and the imidazole ring of His286 were changed into charged species ($C–O^-$ and imidazolium ion, respectively). Direct energy minimizations were then performed with MacroModel/BatchMin in order to optimize the new structures, while maintaining the same set of restraints imposed during the docking.

4.4. Evaluation of differences in free energy of activation

A suitable energy minimization protocol was set up, at both recognition (M–M complexes) and tetrahedral intermediate (THI) formation steps, in which the whole structure of PcL was included, with the aim of estimating (in a qualitative manner) the differences between the free energy of activation of the enantiomers of selected derivatives. Each input complex (enzyme and bound substrate) was put together after having superimposed the so called 'enzyme starting structure' (see above) to the output structure of PcL obtained from the docking, by deletion of the latter (so as to locate the substrate at its proper position into the active site of the former). Geometry optimizations of the complexes were then performed, during which the input structure of PcL was maintained by fixing all the host atoms at their starting positions, with the exception of the side chains of Ser87, Asp264, His286, Glu289, and W510, which were relaxed together with each substrate. In this way unwanted steric energy fluctuations were completely avoided.

Acknowledgements

We thank the 'Centro Universitario per l'Informatica e la Telematica' of the University of Siena and the University of Milan for financial support (to E.S. and S.C.). Support from the Research Training Network (HPRN-CT-2000-00018) is gratefully acknowledged.

References and notes

1. Colombo, G.; Carrea, G. *J. Biotech.* **2002**, *96*, 23–33, and references cited therein.
2. Kazlauskas, R. J. *Curr. Opin. Chem. Biol.* **2000**, *4*, 81–88, and references cited therein.
3. Bornscheuer, U. T. *Curr. Opin. Biotech.* **2002**, *13*, 543–547, and references cited therein.
4. (a) Tuomi, W. V.; Kazlauskas, R. J. *J. Org. Chem.* **1999**, *64*, 2638–2647; (b) Tafi, A.; van Almsick, A.; Corelli, F.; Crusco, M.; Laumen, K. E.; Schneider, M. P.; Botta, M. *J. Org. Chem.* **2000**, *65*, 3659–3665; (c) Gentner, C.; Schmid, R. D.; Pleiss *J. Colloid Surf. B* **2002**, *26*, 57–66; (d) Tomic', S.; Kojic'-Prodic', B. *J. Mol. Graph. Model* **2002**, *21*, 241–252; (e) Guieysse, D.; Salagnad, C.; Monsan, P.; Remaud-Simeon, M.; Tran, V. *Tetrahedron: Asymmetry* **2003**, *14*, 1807–1817.
5. Deslongchamps, P. *Stereoelectronic Effects in Organic Chemistry*; Pergamon: Oxford, 1983.
6. Ema, T.; Kobayashi, J.; Maeno, S.; Sakai, T.; Utaka, T. *Bull. Chem. Soc. Jpn.* **1998**, *71*, 443–453.
7. Ema, T.; Jittani, M.; Furuie, K.; Utaka, M.; Sakai, T. *J. Org. Chem.* **2002**, *67*, 2144–2151.
8. Dugas, H. *Bioorganic Chemistry. A Chemical Approach to Enzyme Action*, 3rd ed.; Springer: New York, 1996; Chapter 4.
9. A relaxed structure of PcL, the so called 'enzyme starting structure (see Experimental), has been fully included and kept invariably steady during these minimizations by fixing all the enzyme atoms at the positions they occupied in the input structure, with the exception of the side chains of Ser87, Asp264, His286, Glu289, and W510, which were relaxed together with each substrate. In this way the uncontrollable and unwanted steric energy fluctuations, previously detected by other authors in the same kind of calculations,[2,4a] have been completely avoided furnishing an original solution to the challenging task of the energy evaluation of enzyme–substrate complexes.
10. Ferraboschi, P.; Casati, S.; De Grandi, S.; Grisenti, P.; Santaniello, E. *Biocatalysis* **1994**, *10*, 279–288.
11. Tomic', S.; Dobovicnik, V.; Sunjic', V.; Kojic'-Prodic', B. *Croat. Chem. Acta* **2001**, *74*, 343–357.
12. Dale, J. A.; Dull, D. L.; Mosher, H. S. *J. Org. Chem.* **1969**, *34*, 2543–2549.
13. Chen, C.-S.; Fujiimoto, Y.; Girdaukas, G.; Sih, C. J. *J. Am. Chem. Soc.* **1982**, *104*, 7294–7299.
14. The software package InsightII of Accelrys, San Diego, CA, USA was used to perform the graphics manipulations.

15. Lang, D. A.; Mannesse, M. L. M.; De Haas, G. H.; Verheij, H. M.; Dijkstra, W. *Eur. J. Biochem.* **1998**, *254*, 333–340.
16. On this subject it has to be noted that, when the THIs deriving from the global minimum recognition geometry of (S)-**1d** and (*R*)-**1d** were optimized, the *gauche-anti* enantioselective differentiation of the alcoholic moiety, already described for **1b**, was observed again. Some M–M complexes of (*S*)-**1d** were found however (at energy values very close to the global minimum), whose acyl chains were occupying the HA binding pocket with slightly different folding patterns, in accordance with the observation that HA snugly accommodates fatty acid chains.[15] When a few of these geometries were transformed into the corresponding THI's and relaxed, an *anti*-conformation of the alcoholic moiety was detected, probably due to propagation of the perturbation caused by the rearrangement of the acyl chain into HA. Such a *gauche-anti* conformational interconversion, if real, would be even more effective in slowing down the reaction speed of the fast-reacting enantiomer in light of the stereoelectronic theory requirements (see the third column of Table 2). A similar overall picture—not discussed in the text—was obtained too, when the hydrolysis of **1e** was simulated.
17. Haeffner, F.; Norin, T.; Hult, K. *Biophys. J.* **1998**, *74*, 1251–1262.
18. The ΔE values reported in the second column of Table 2 suggest a steady preference of PcL towards the (*R*)-enantiomers of the primary alcohols during the recognition step. The trend of these data—related to the experimentally observed drop of enantioselectivity—could be interpreted as a further sign that lipase enantioselectivity does not come into play during the recognition process.
19. Schrag, J. D.; Li, Y.; Cygler, M.; Lang, D.; Burgdorf, T.; Hecht, H.-J.; Schmid, R.; Schomburg, D.; Rydel, T. J.; Oliver, J. D.; Strickland, L. C.; Dunaway, M. C.; Larson, S. B.; Day, J.; McPherson, A. *Structure* **1997**, *5*, 187.
20. Mohamadi, F.; Richards, N. G. J.; Guida, W. C.; Liskamp, R.; Lipton, M.; Caufield, C.; Chang, G.; Hendrickson, T.; Still, W. C. *J. Comp. Chem.* **1990**, *11*, 440.
21. McDonald, D. Q.; Still, W. C. *Tetrahedron Lett.* **1992**, *33*, 7743.
22. Still, W. C.; Tempczyk, A.; Hawley, R. C.; Hendrickson, T. *J. Am. Chem. Soc.* **1990**, *112*, 6127.